Electronic Supplementary Information

Hydrogel Adhesive Formed via Multiple Chemical Interactions: From Persistent Wet Adhesion to Rapid Hemostasis

Min Liang,[‡] Dandan Wei,[‡] Zhangyu Yao,[§] Pengfei Ren,[‡] Jidong Dai,[‡] Li Xu,[‡] Tianzhu Zhang,* Qianli Zhang[†]

[‡]State Key Lab of Bioelectronics, National Demonstration Center for Experimental Biomedical Engineering Education, School of Biological Science and Medical Engineering, Southeast University, Nanjing 210096, China.

[§]Department of Head and Neck Surgery, The Affiliated Cancer Hospital of Nanjing Medical University, Nanjing 210009, China.

[†]School of Chemistry and Life Science, Suzhou University of Science and Technology, Suzhou 215009, China.

*Corresponding author: zhangtianzhu@seu.edu.cn (Tianzhu Zhang)

EXPERIMENTAL DETAILS

Materials

Acrylic acid (AAc), chitosan (CS, ≥75% deacetylated, low viscosity, 100~200 mPa.s), tannic acid (TA), *N, N′*-methylene bis-acrylamide (MBAm), ammonium persulfate (APS), 4-Morpholineethanesulfonic acid (MES), *N*-(3-Dimethylaminopropyl)-*N′*-ethylcarbodiimide hydrochloride (EDC), *N*-Hydroxysuccinimide (NHS), agarose and all inorganic salts were purchased from Aladdin Industrial Inc. (Shanghai, China). Phosphate Buffered Saline (PBS) dry powder (0.01 M, pH 7.2~7.4) purchased from Biosharp Life Sciences Co., Ltd. (Anhui, China) was used for testing in non-sterile environment. Mouse fibroblast cell lines (L929) and human umbilical vein endothelial cell lines (HUVEC) were obtained from Stem Cell Bank of Chinese Academy of Sciences (China). Triton X-100, Dulbecco's Modified Eagle Medium (DMEM), Roswell Park Memorial Institute 1640 Medium (RPMI-1640), PBS (pH 7.4), 0.25% trypsin-EDTA, lactate dehydrogenase (LDH) assay kit, CCK-8 cell viability assay kit, live/dead cell staining kit were purchased from KeyGen Biotechnology Co., Ltd. (Jiangsu, China). Fetal bovine serum (FBS) was obtained from Gibco (USA). Porcine fibrin sealant kit was obtained from Bioseal Biotechnology Co., Ltd. (Guangzhou, China). All chemicals were commercially available, and used without further purification. All fresh tissues for in vitro experiments were purchased from local food market (Jinxianghe market, Jiangsu, China).

Preparation of Hydrogel matrixes

To prepare PAAc/CS/TA hydrogels, a deionized aqueous solution of AAc (20~40 vol.%), CS (0~5 wt%) and MBAm (0~0.8 mg/mL) were first obtained. TA (0~5 wt%) was subsequently dissolved in the above-mentioned solution under stirring for 30 min at 50 °C. After that, APS solution (8 mg/mL) was added dropwise to the mixed solution under stirring at 50 °C. Finally, the mixture was poured on a sealed polytetrafluoroethylene mould for further polymerization in an incubator for 1 h at

60 °C. The hydrogels were named as $P_xC_yT_z$ ($MBAm_n$), where subscripts x, y, z, and n denote the concentration of AAc (vol.%), CS (wt%), TA (wt%) and MBAm (mg/mL), respectively (Table S1).

Besides, P, PC, PT, and CT hydrogel represent PAAc, PAAc/CS, PAAc/TA, and CS/TA hydrogel, respectively. The preparation of these hydrogels was similar to that of $P_{30}C_3T_3$ ($MBAm_{0.6}$) hydrogel, except for the absence of some components.

Table S1. The preparation formula of Hydrogel Matrixes.

Chemicals Hydrogels	Deionized water (mL)	AAc (mL)	CS (g)	20 mg/mL MBAm solution (mL)	TA (g)	0.4 g/mL APS solution (mL)	Water content (%)
P	10	3	——	0.3	——	0.2	75.97
PC	10	3	0.3	0.3	——	0.2	74.34
PT	10	3	——	0.3	0.3	0.2	74.34
CT	10	3	0.3	——	0.3	0.2	74.37
$P_{30}C_3T_3$ ($MBAm_{0.2}$)	10	3	0.3	0.1	0.3	0.2	73.87
$P_{30}C_3T_3$ ($MBAm_{0.4}$)	10	3	0.3	0.2	0.3	0.2	73.32
$P_{30}C_3T_3$ ($MBAm_{0.6}$)	10	3	0.3	0.3	0.3	0.2	72.79

Preparation of Hydrogel-Tissue Adhesive Interface

To prepare a hydrogel-tissue adhesive interface, the surface of tissues was treated with the bridging agent composed of bridging polymer and coupling agents for carbodiimide coupling reaction. CS (2 wt%) was selected to serve as the bridging polymer, and EDC/NHS was used as the coupling agents. CS was dissolved in MES buffer (0.1 M) and the pH was adjusted to 6. EDC (1.2 wt%) and NHS (1.2 wt%) were subsequently dissolved in the above-mentioned solution. Finally, the mixture (~100 µL) was evenly applied to the interface between the tissue and the hydrogel matrix (60 mm of length, 20 mm of width), and then placed at 25 °C for 20 min to construct the multiple bonded adhesive interface.
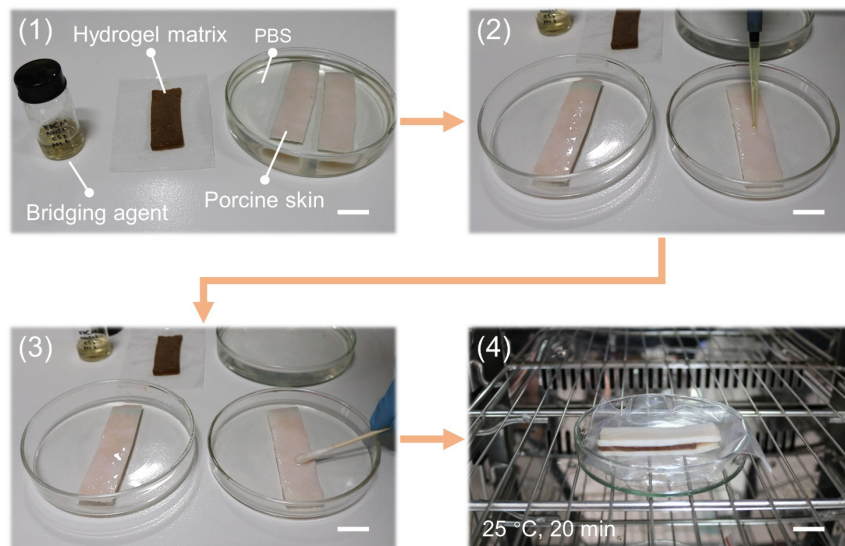
Figure S1. Stepwise preparation photographs of hydrogel-tissue adhesive interface. Porcine skin was used as a representative tissue for demonstration. The scale bar represents 2 cm.

Structural and Morphological Characterization of Hydrogels

Structural analysis of hydrogel adhesives was performed using a Fourier transform infrared (FTIR) spectrometer (Nicolet 5700, Thermo Fisher Scientific, America). The microstructure and surface morphology of cross-sections of the freeze-dried hydrogels was observed using a field emission scanning electron microscope (FE-SEM, Ultra Plus, Carl Zeiss, Germany). The UV-vis spectra of hydrogel components were recorded using a spectrophotometer (Alpha-1900PC, China) in the range of 190-600 nm. Thermogravimetric analysis (TGA) was performed using a TG209 F3 (NETZSCH, Germany) instrument with heating ramps of 30 °C min^{-1} in the temperature range from 30 to 600 °C.

Swelling Behavior

The as-prepared hydrogel samples (cylinder, 7.6 mm of diameter, 5 mm of height) were immersed in PBS (0.01 M) or deionized water (DIW), and weighed at specific time to investigate swelling behavior via the traditional swelling method at 37 °C. The swelling ratio was defined as follows (N = 5)

$$\text{Swelling Ratio}(\%) \ = \ \frac{W_s - W_i}{W_i} \times 100\% \qquad (1)$$

where W_s and W_i are the weight of the swelling samples at a given time and the as-prepared samples, respectively.

Rheological Measurement

Dynamic rheological properties of the hydrogel samples (cylinder, 25 mm of diameter, 1 mm of height) were characterized at 25 °C using a strain-controlled rheometer equipped with 25 mm parallel plates (MCR 302, Anton Paar, Austria). The dynamic frequency sweeps were performed in the linear viscoelastic region of materials at 0.5 % strain amplitude. The loss factor (tanδ) was defined as the ratio of loss modulus (G") to storage modulus (G').

Mechanical Test

The hydrogel samples (cuboid, 40 mm of length, 25 mm of width, 1~3 mm of thickness) with a spacing of the clamps of 10 mm were prepared to perform the tensile tests (FLR-303, Flora Automatic Technology, China) at the speed of 5 mm·min^{-1} (N = 5). The nominal stress is the applied force divided by the cross-sectional area of the undeform sample. The strain is the length of deformed sample divided by the initial length. The elastic modulus of tensile samples was obtained by calculating the slope of the stress-strain curve in the linear region.

Adhesion Test

All engineering solids were pretreated by rinsing with ethanol and deionized water and then dried before test. All fresh porcine tissues were cleaned with deionized water to remove superfluous fat or blood before test. The shear strength, interfacial toughness and tensile strength of hydrogel matrixes was investigated by the standard lap-shear test (ASTM F2255), the standard peel test (ASTM F2256 for 180-degree peel test, and ASTM D2861 for 90-degree peel test) and the standard tensile test (ASTM F2258), respectively (Figure. S2). All tests were conducted with a constant tensile speed of 10

mm·min^{-1} by a tensile testing machine (FLR-303, Flora Automatic Technology, China) (N = 5).
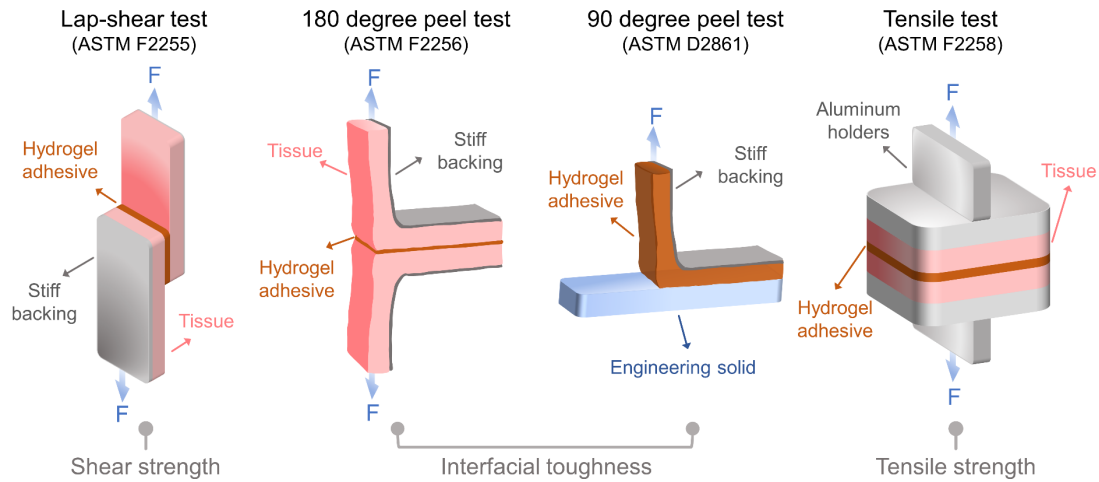
Figure S2. Setups for mechanical testing of adhesion performance

To measure shear strength, the as-prepared hydrogel (25 mm of length, 25mm of width) was adhered immediately between two porcine skin tissues to prepare the lap-shear joint. Double sided tapes were applied using cyanoacrylate glues to act as a stiff backing for the adhered substrates and hydrogels. Shear strength was defined as the ratio of maximum tensile force to the adhesion area.

To measure interfacial toughness, the as-prepared hydrogel (100 mm of length, 25 mm of width) was adhered immediately to the surface of different engineering solids or porcine tissues. Double sided tapes were applied using cyanoacrylate glues to act as a stiff backing for the adhered substrates and hydrogels. Interfacial toughness was defined as the ratio of two times the plateau force (for a 180-degree peel test) or the plateau force (for a 90-degree peel test) to the width of the hydrogel samples.

To measure tensile strength, the as-prepared hydrogel (25 mm of length, 25mm of width) was adhered immediately between two porcine skin tissues. Aluminium holders were applied using cyanoacrylate glues to provide grips for tests. To provide a wet environment, the PBS was dropped at the interface between the hydrogel and skin tissues. To investigate the effects of contact time and preload strength on the tensile strength, the applying preload was set to 5, 10, 20, 30, 50, 100, 150, 200 kPa with a contact time of 30 s, or the contact time was varied from 5 to 600 s with a preload of 100 kPa. After being compressed with the preload, the two surfaces were separated.

Tensile strength was defined as the ratio of the maximum debonding force by the adhesion area.

Blood Compatibility Evaluation

All animal procedures were performed in accordance with the Guidelines for Care and Use of Laboratory Animals of Southeast University in China and approved by the Animal Ethics Committee of Southeast University in China. Fresh rabbit's whole blood with sodium citrate solution (3.8 wt%) was centrifuged to separate red blood cells (RBCs) and platelet-rich plasma (PRP) for a hemolysis assay and to evaluate platelet adhesion to the hydrogel samples, respectively.

To evaluate the hemolysis effect of the hydrogels, 250 μL of diluted RBCs (1 mL of RBCs with 11.5 mL of normal saline) was added to pre-swollen equilibrium hydrogels (50 mg of dry weight) in separate centrifuge tubes. The same volume of deionized water and normal saline without hydrogels were used as positive and negative controls, respectively. The hydrogels were removed from tubes after being incubated at 37 °C for 1 h, and then the tubes were centrifuged at 3000 rpm for 10 min. The absorbance of the obtained supernatant was measured using a microplate reader at 562 nm. The hemolysis rate was calculated by the following eq (N = 3).

$$\text{Hemolysis rate (\%)} = \frac{A_s - A_{nc}}{A_{pc} - A_{nc}} \times 100 \tag{2}$$

Where A_s, A_{nc}, and A_{pc} represent the absorbance of hydrogel sample groups, negative control groups and positive control groups, respectively.

To evaluate platelet adhesion effect on the surface of hydrogels, 2 mL of PRP suspension was added to pre-swollen equilibrium hydrogels (10 mg of dry weight) in 24-well plates. After incubating at 37 °C for 1 h, the hydrogels were gently washed thrice with PBS and immersed in 2.5% glutaraldehyde solution for 2 h to fix platelets on the surface of hydrogels. Then, the hydrogels were again washed thrice with PBS and dehydrated in gradient ethanol solutions (30, 50, 70, and 100%). Finally, the morphology of the adherent platelets was observed by FE-SEM (Ultra Plus, Carl Zeiss, Germany). Furthermore, the LDH assay was used to quantify the adherent platelets on

the surface of hydrogels. The above-mentioned dehydrated hydrogel samples with adherent platelets were lysed by incubating with 1% Triton X-100 at 37 °C for 1 h. The lysate was analysis using LDH assay kit according to manufacturer's instructions. The hydrogels treated with PBS instead of PRP were used as blank groups. The normalized absorbance of LDH obtained by subtracting the absorbance of the blank group from the absorbance of the hydrogel group was correlated to the number of platelets adhered to the samples (N = 5).

To evaluate in vitro dynamic coagulation effect of hydrogels, 20 μL of 0.2 M $CaCl_2$ solution was quickly mixed with 250 μL of whole blood, and then pre-swollen equilibrium hydrogels (10 mg of dry weight) was immediately added to the mixture. After incubating at 37 °C at the shaking speed of 30 rpm for specific times (5, 10, 20 and 30 min), the mixture was mixed with 50 mL of deionized water to hemolyze the red blood cells that are not entrapped in blood clots. The absorbance of the obtained supernatant was measured using a microplate reader at 562 nm. The same volume of whole blood with $CaCl_2$ solution in deionized water without hydrogels were used as control group. The blood clotting index (BCI) was defined as the ratio of the absorbance of the hydrogel groups to the absorbance of the control group (N = 3).

In Vitro Cytocompatibility Evaluation

In vitro cytocompatibility of hydrogels were evaluated by the cytotoxicity of degradation medium, extraction medium, and bulk of hydrogels, as well as attachment on the surface of hydrogels, respectively. L929 and HUVEC were cultured in DMEM and RPMI-1640 supplemented with 10 wt% FBS and 100 U·mL^{-1} penicillin/streptomycin at 37 °C in 5% CO_2 for all subsequent cell experiments, respectively.

Degradation Medium Test: Briefly, 15 mg of freeze-dried $P_{30}C_3T_3$ ($MBAm_{0.6}$) hydrogel were swollen in daily replaced PBS for 7 days. Subsequently, the hydrogel was soaked in 15 mL of PBS and kept in an incubator at 37 °C shaking at 80 rpm for up to 4 weeks and 8 weeks, respectively. The medium was filtered through 220 μm of filter membrane before test. A count of 1×10^4 cells per well were seeded into a 96-

well plate (180 μL/well) and incubated with the degradation medium (20 μL/well). The same amount of cell suspension and PBS was used as a control.

Extraction Medium Test: The hydrogel samples were purified by PBS, 75% ethanol, and supplemented medium. To prepare the extraction medium, the hydrogel was incubated in supplemented medium at 37 °C for 24 h (200 mg/mL), and then the medium was filtered through 220 μm of filter membrane before test. A count of 1×10^4 cells per well were seeded into a 96-well plate (100 μL/well) and incubated with the extraction medium (100 μL/well). The same amount of cell suspension and supplemented medium was used as a control.

Bulk of Hydrogel Test: The hydrogel samples were purified by PBS, 75% ethanol, and supplemented medium. A count of 1×10^4 cells per well were seeded into a 96-well plate (200 μL/well) and incubated with 5 mg of hydrogel (cube, 2 mm of length, 2 mm of width, 2 mm of height). Cell suspension without co-culturing the hydrogel was used as a control.

Cell Attachment Test: The hydrogel samples were purified by PBS, 75% ethanol, and supplemented medium. Subsequently, the hydrogel (cylinder, 6 mm of diameter, 2 mm of thickness) was placed at the bottom of a 96-well plate, and the edge was sealed with agarose hydrogel (2 wt%) to prevent the cell suspension from leaking to the bottom. A count of 1×10^4 cells per well were seeded into the surface of hydrogel (100 μL/well). Cell adhesion on the surface of agarose hydrogel was used as a control.

After 1, 3, 5, and 7 days of culture, the cell viability was determined by the CCK-8 kit and the live/dead cell staining kit. The fluorescent images were photographed by an inverted microscope (MShot, MF52, China). The absorbance of the solution was measured using a Microplate Reader (Multiskan FC, Thermo, America) at 450 nm. The cell viability was calculated by the following eq (N = 5)

$$\text{Relative Cell Viability (\%)} = \frac{A_s - A_b}{A_c - A_b} \times 100 \qquad (3)$$

Where A_s, A_c, and A_b represent the absorbance of sample groups, control groups and blank groups, respectively.

Burst Pressure Measurement

To evaluate the efficacy of the hydrogel as a tissue sealant, a burst pressure test was carried out using a designed apparatus. Briefly, all fresh porcine tissues were cleaned with deionized water to remove superfluous fat or blood before test. Subsequently, a combination of tissue and tube with a hole (2 mm of diameter) was sealed with the as-prepared hydrogel (7.6 mm of diameter, 2 mm of thickness). A syringe filled with air or rhodamine B stained PBS pressurize the sealing apparatus at a speed of 2 mm/min. The maximum burst pressure was recorded using a digital pressure gauge (FK-Y810, Fullkon, China) (N = 10).

In vivo Hemostatic Effect

The hemostatic ability of the commercial fibrin glue, the PAAc hydrogel, and the injectable $P_{30}C_3T_3$ ($MBAm_{0.2}$) hydrogel was evaluated by employing a rat liver trauma model. All animal procedures were performed in accordance with the Guidelines for Care and Use of Laboratory Animals of Southeast University in China and approved by the Animal Ethics Committee of Southeast University in China. Sprague-Dawley rats (200~250 g) were fixed on the surgical board after anesthesia, and the board was kept at an included angle of 30° with the horizontal plane. The liver of the rat was exposed by abdominal incision, and serous fluid around the liver was carefully removed. A pre-weighed filter paper on a paraffin film was placed beneath the liver, and bleeding was induced using a 20-gauge needle. Afterward, the P hydrogel (cylinder, 10 mm of diameter, 3 mm of height), ~200 μL of the fibrin glue, and ~200 μL of the PCT hydrogel was immediately applied to the bleeding site, respectively. Groups without any treatment were used as blank controls. The accumulated amount of the blood loss was recorded by weighing the filter papers after 120 s (N = 5).

Statistical Analysis

Statistical analysis of data was performed by one-way analysis of variance (ANOVA) using IBM SPSS 23.0 software. Post hoc comparisons were performed using Tukey's honest significant difference (HSD) test to compare means of multiple groups. Results

were expressed as mean ± standard deviation, with *p* values < 0.05 indicating significance.
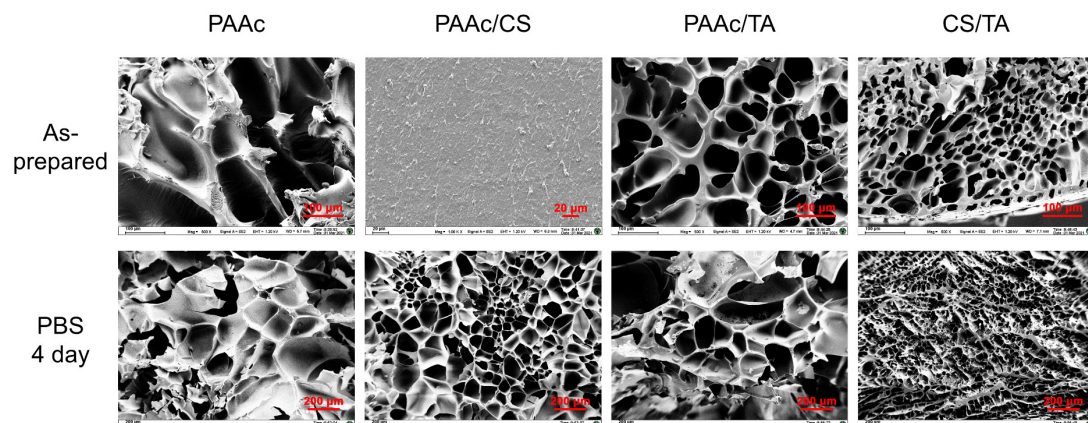
Figure S3. The SEM images of the cross-section micromorphology of the P, PC, PT, and CT hydrogels before and after swelling in PBS for 4 days.
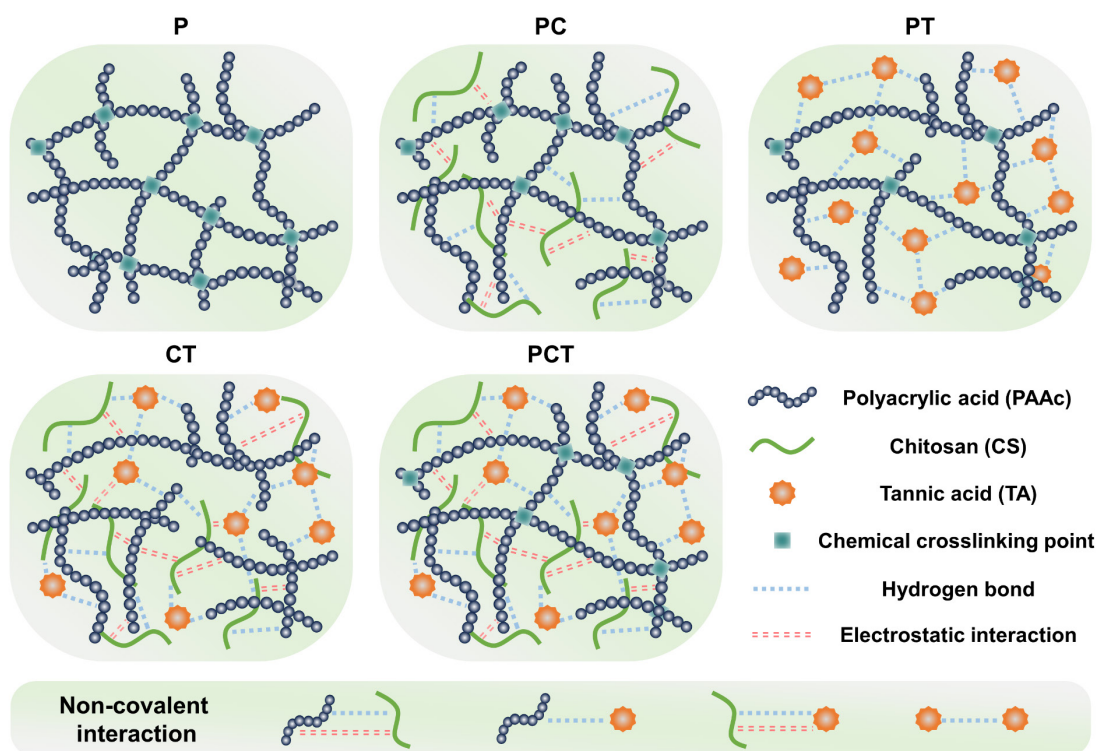
Figure S4. Schematic structure of the related composite hydrogels, namely, the P, PC, PT, CT and PCT hydrogel.

Table S2. The corresponding characteristic peak in FTIR spectra of hydrogel components.

Component	Wavenumber (cm^{-1})	Assignment	Reference
PAAc	3429	stretching vibration of O−H	1, 2
	1719	stretching vibration of C=O	3
	1560/1410	asymmetric and symmetric stretching vibration of the carboxylate group	4
	1250/1166	stretching vibration of C−O	3
CS	3427	stretching vibration of O−H	5
	3280	O−H stretching overlapping the N−H stretching	6
	2875	stretching vibration of C−H	5-7
	2364	asymmetric stretching vibration of C−N	8
	1653	stretching vibration of C=O, amide I	5, 8
	1597	bending vibration of −NH$_2$	6
	1383	asymmetric C−H bending of −CH$_2$	6, 8
	1155	asymmetrical stretching vibration of C−O−C bridge	5, 6
	1075	stretching vibration of C−O	5, 8
	1050	stretching vibration of C−OH	7
TA	3369	stretching vibration of O−H	9
	2710	asymmetric stretching vibration of C−H	10
	1717	stretching vibration of C=O	3, 10
	1612	stretching vibration of aromatic C−O	9, 10
	1534/1518/1447	aromatic C=C	10
	1317	in-plane bending vibration of phenol groups	2
	1321/1198	asymmetric stretching vibration of aromatic C−O	10
	1029	stretching vibration of C−O−C	9, 10
	758	out-of-plane deformation of C−H	10
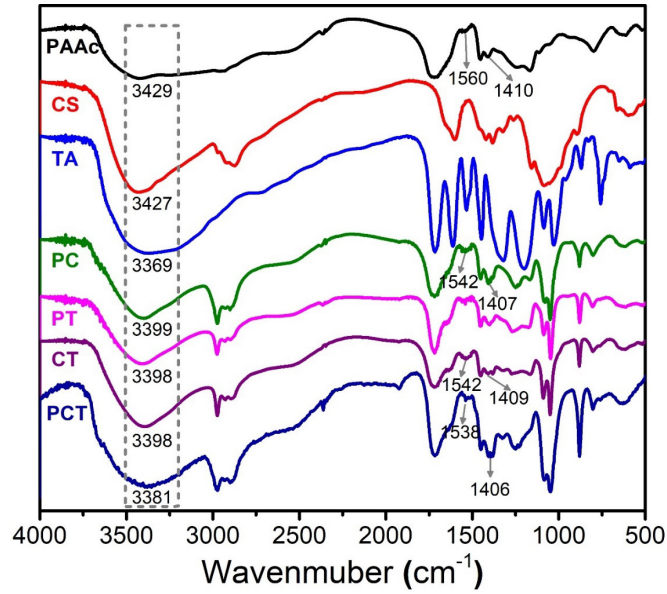
Figure S5. The FTIR spectra of hydrogel components.

For the PC hydrogel, the two peaks at 1542 cm^{-1} and 1407 cm^{-1}, were indicative of the asymmetric and symmetric stretching vibration of the carboxylate group, respectively. Those two peaks shifted toward low frequency compared with the P hydrogel, indicating that the formation of electrostatic interactions between PAAc and CS. Similar phenomena were found in the curve of the PCT hydrogel compared to the curve of the CT hydrogel. For the PCT hydrogel, the characteristic peak of the O−H stretching vibration shifted toward low frequency in comparison to the single or dual components, indicating that the formation of hydrogen bonds between the components.
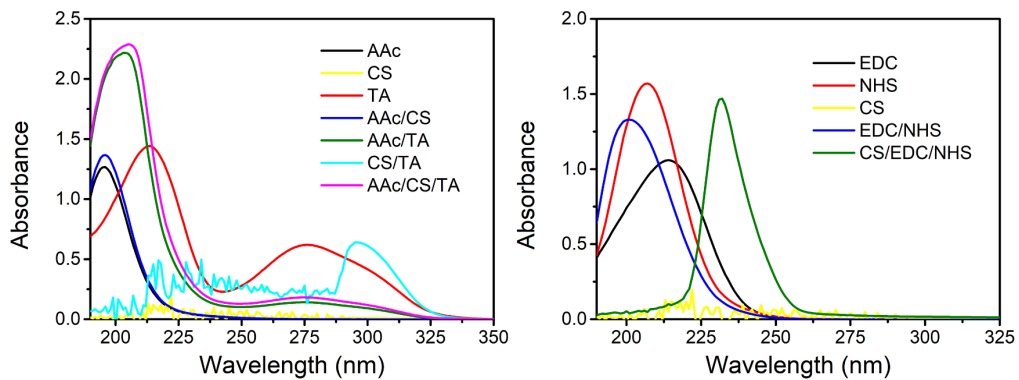
Figure S6. The UV-vis spectra of the components of the hydrogel matrix and the hydrogel adhesive.
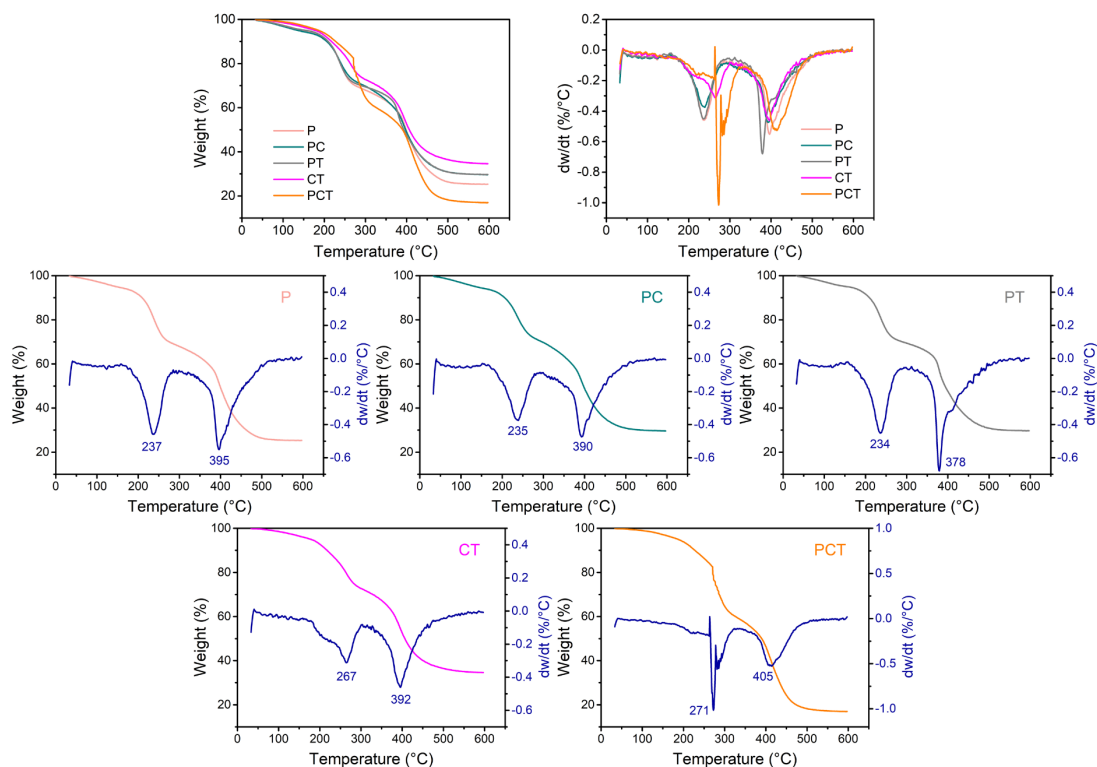
Figure S7. Thermogravimetric analysis (TGA) curves and differential thermogravimetry (DTG) curves of the P, PC, PT, CT, and PCT hydrogel.

The related composite hydrogels all exhibited two-step degradation with similar thermal behavior. The first maximum pyrolysis temperatures of the P, PC, PT, CT, and PCT hydrogel are 237 °C, 235 °C, 234 °C, 267 °C and 271 °C, respectively. The second maximum pyrolysis temperatures of the P, PC, PT, CT, and PCT hydrogel are 395 °C, 390 °C, 378 °C, 392 °C and 405 °C, respectively. Decomposition of the PCT hydrogel shifted to a higher temperature, indicating that the non-covalent interactions inside the hydrogel network enhanced thermal stability.
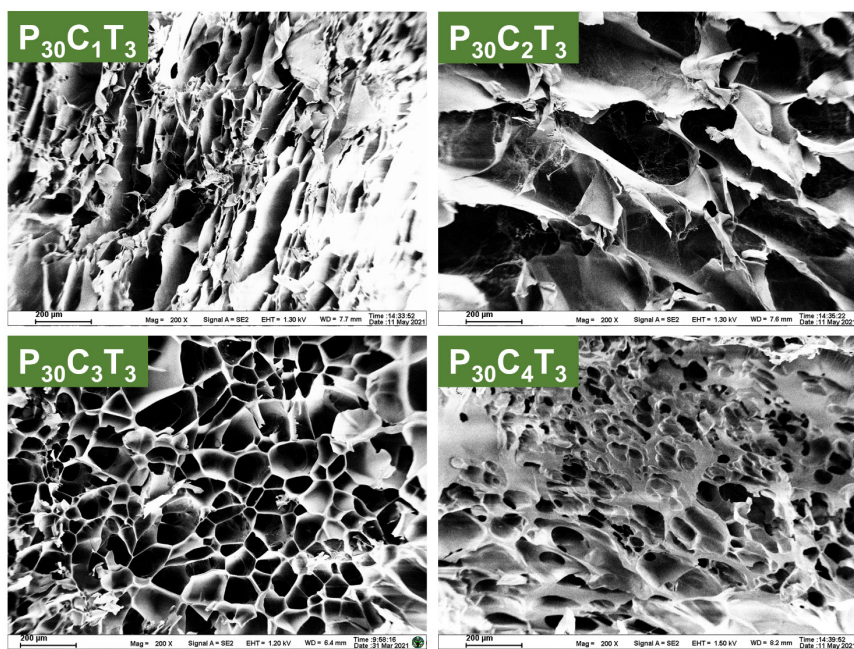
Figure S8. The SEM images of the cross-section micromorphology of the $P_{30}C_xT_3$ (MBAm$_{0.6}$) hydrogels with different concentration of CS after swelling in deionized water for 4 days.
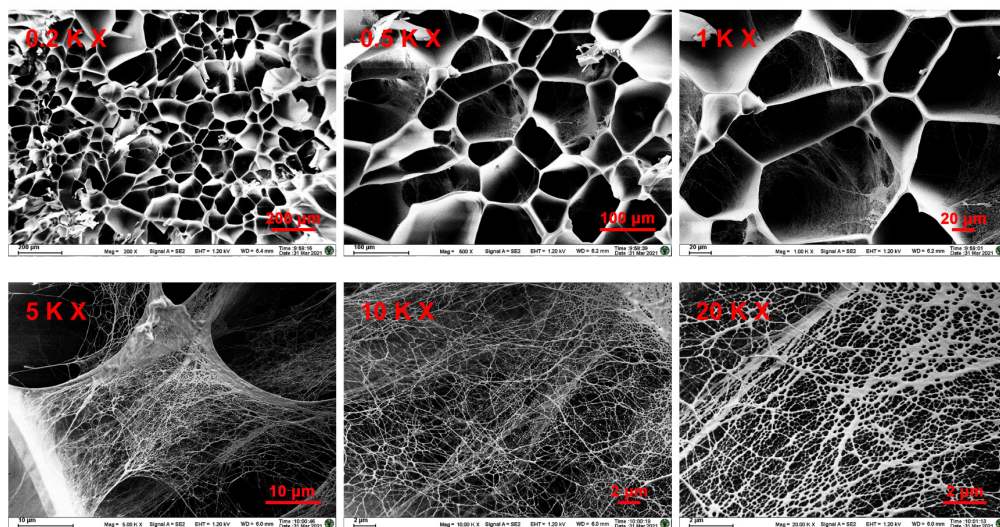
Figure S9. The SEM images of the cross-section micromorphology of the swollen $P_{30}C_3T_3$ (MBAm$_{0.6}$) hydrogel in deionized water for 4 days with different magnification times.
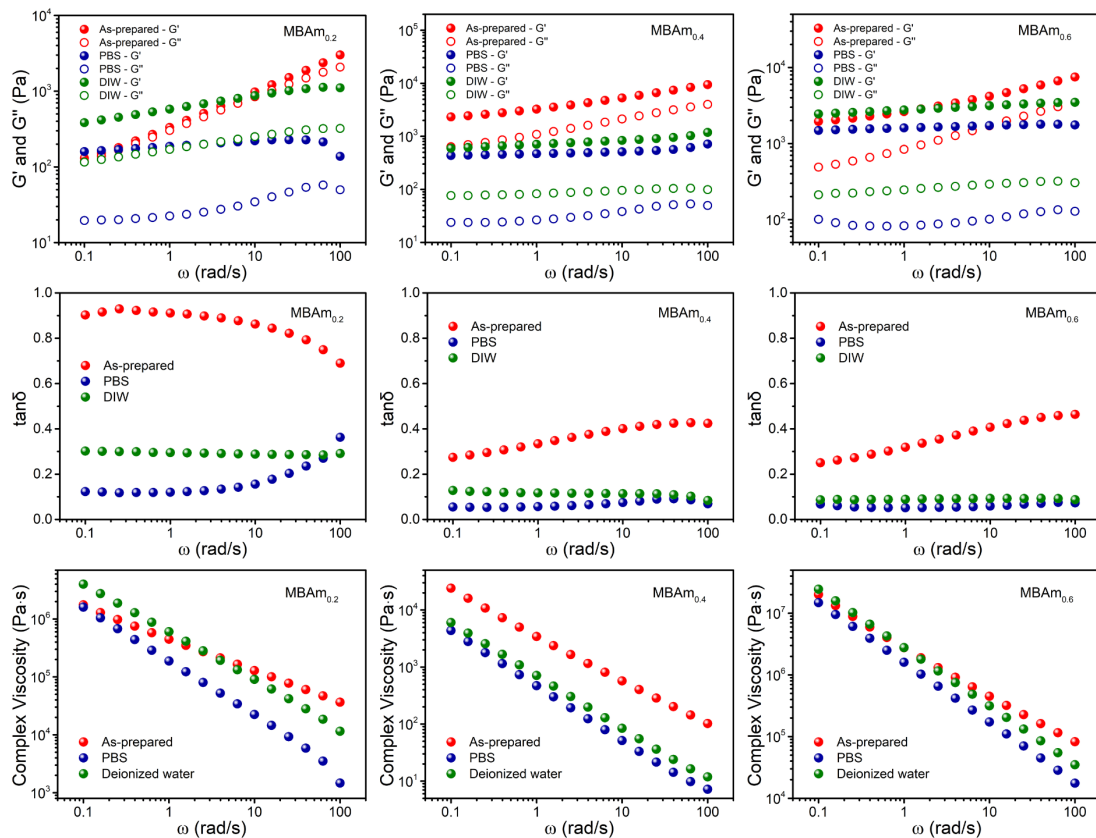
Figure S10. Storage modulus (G′), loss modulus (G″), loss factor (tanδ), and complex viscosity of the $P_{30}C_3T_3$ hydrogels with different concentration of MBAm before and after swelling in PBS or deionized water for 4 days.
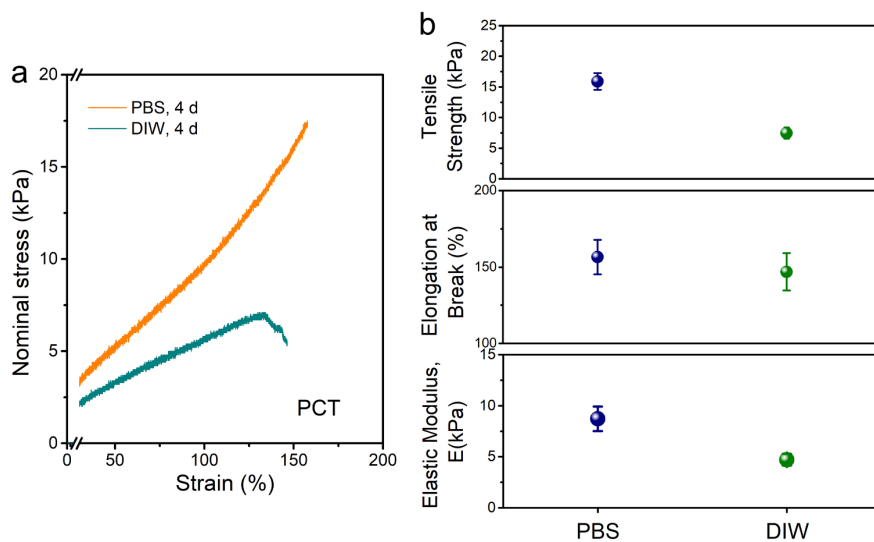
Figure S11. (a) Tensile stress-strain curves of the swollen $P_{30}C_3T_3$ (MBAm$_{0.6}$) hydrogels in PBS and deionized water for 4 days, respectively. (b) Comparison of tensile strength, elongation at break and elastic modulus of the swollen PCT hydrogels.
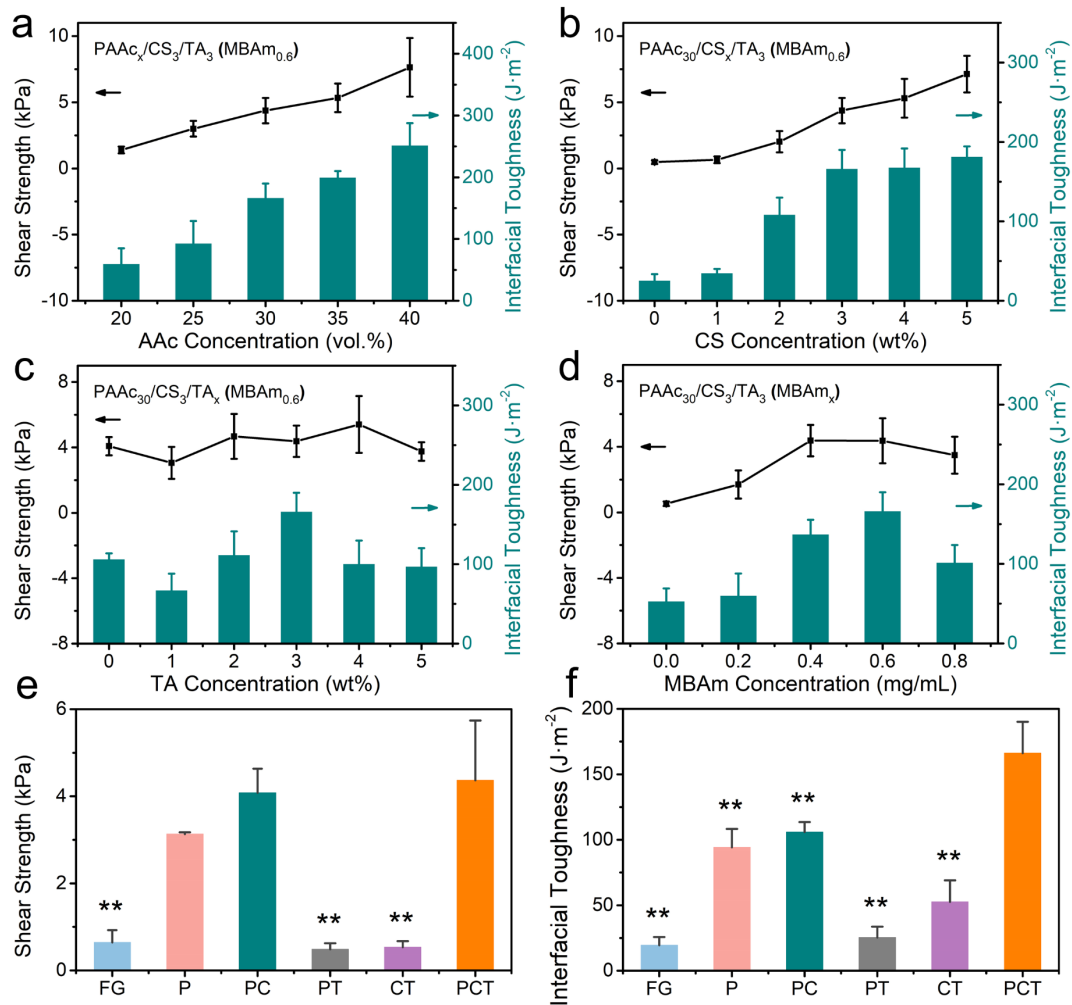
Figure S12. Shear adhesion strength and interfacial toughness of hydrogel matrixes with different concentrations of (a) AAc, (b) CS, (c) TA and (d) MBAm adhered to porcine skin in dry environment. (e) shear adhesion strength and (f) interfacial toughness of the commercial fibrin glue and the related composite hydrogels adhered to porcine skin in dry environment. $^{**}p < 0.01$, vs. shear adhesion strength or interfacial toughness of the PCT hydrogel group.
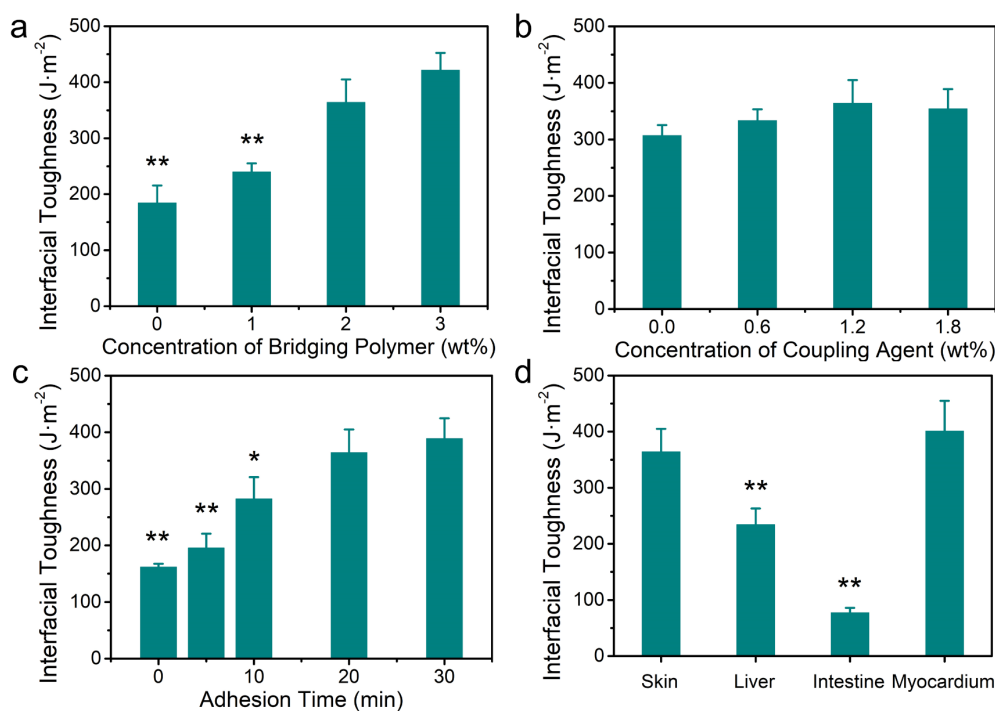
Figure S13. Interfacial toughness of the hydrogel-tissue adhesive interface with different (a) concentrations of bridging polymer, (b) concentrations of coupling agent, (c) reaction times, and (d) tissue substrates in dry environment. Unless otherwise specified, the default concentration of bridging polymer, concentration of coupling agent, adhesion time, and tissue substrate was 2 wt%, 1.2 wt%, 20min and porcine skin, respectively. $*p < 0.05$, $**p < 0.01$, vs. the interfacial toughness of the experimental group with the maximum value under the same test conditions.
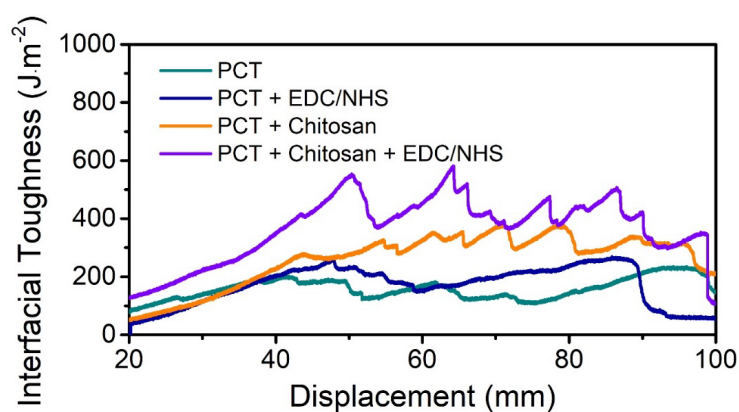
Figure S14. Interfacial toughness-displacement curve of the hydrogel adhesive in dry environment. The concentration of CS, concentration of EDC/NHS, adhesion time, and tissue substrate was 2 wt%, 1.2 wt%, 20min and porcine skin, respectively.
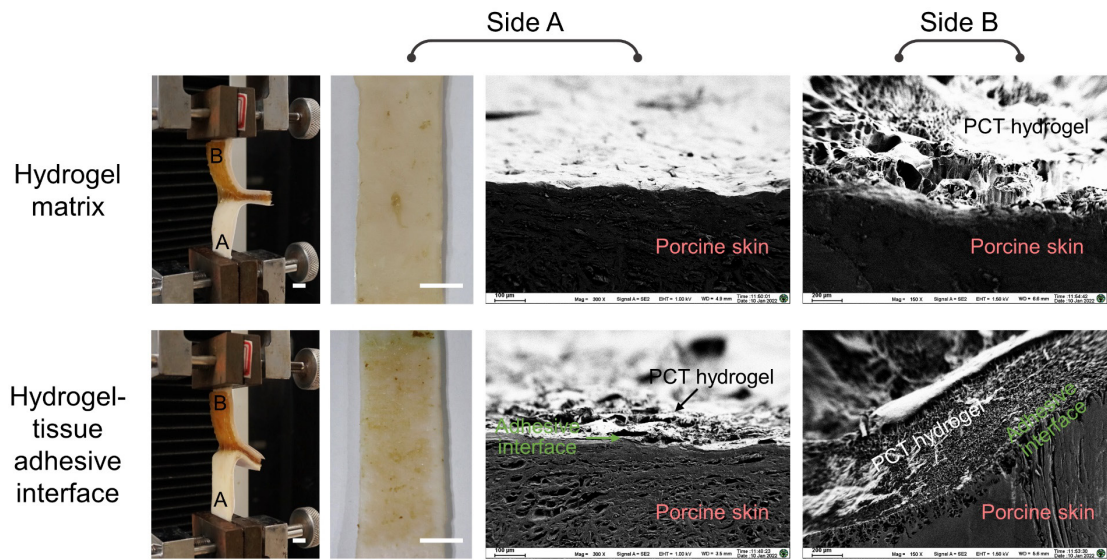
Figure S15. Optical images and SEM images of cross-section micromorphology of the porcine skin after peeling test. The scale bar in the optical images represents 1 cm.

Table S3. Comparison of adhesion properties for the existing hydrogel adhesives published in the literature.

Hydrogel adhesives	Time to achieve firm adhesion (substrate)	Repeatability of wet adhesion (test method, substrate, cycles, adhesion)	Durability of underwater adhesion (test method, substrate, time, adhesion)
This work	5 sec (porcine skin)	✓ (tensile test, porcine skin, 50, 68 kPa)	✓ (180 degree peel test, porcine skin, 30 days, 90 J·m^{-2})
Fan HL, et al. Adv. Funct. Mater. 2020[11]	10 sec (glass)	✓ (tack test, glass, 50, ~ 32 N)	✓ (lap-shear test, glass, 100 days, ~ 175 kPa)
Su X, et al. Mater. Horiz. 2020[2]	10 sec (porcine skin)	✓ (lap-shear test, porcine skin, 5, ~ 15 kPa)	✓ (lap-shear test, porcine skin, 1 days, ~ 6 kPa)
Han L. et al. Adv. Funct. Mater. 2019[12]	2 min (polypropylene)	✓ (tensile test, polypropylene, 50, ~ 50 kPa)	✓ (tensile test, polypropylene, 7 days, ~ 30 kPa)
Yu ZC, et al. Mater. Horiz. 2021[13]	5 min (glass)	N/R	✓ (lap-shear test, glass, 60 days, ~ 5 MPa)
Cui CY, et al. Adv. Funct. Mater. 2020[14]	Instantly (porcine skin)	N/R	✓ (180 degree peel test, porcine skin, 8 hours, ~ 150 J·m^{-2})
Pan F, et al. Mater. Horiz. 2020[15]	N/R	N/R	✓ (lap-shear test, aluminum, 7 days, ~ 3000 kPa)
Xu LJ, et al. Adv. Mater. 2020[16]	N/R	N/R	✓ (lap-shear test, glass, 7 days, ~ 300 kPa)
Lee JN, et al. ACS Appl. Mater. Interfaces 2021[17]	1 h (porcine skin)	N/R	N/R
Yuk H, et al. Nature 2019[18]	5 sec (porcine skin)	N/R	N/R

*N/R means not reported. Note that despite the data presented, the adhesion may vary largely because of differences in measuring conditions.
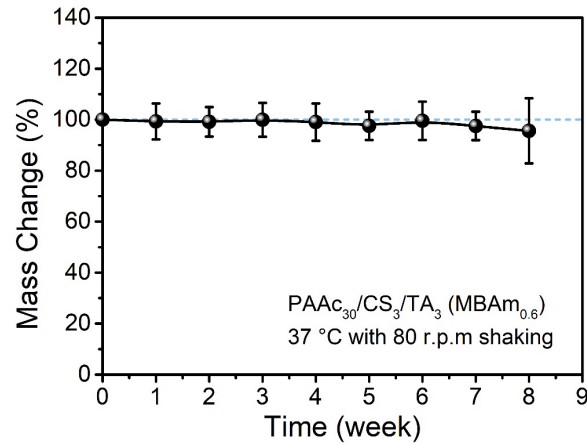
Figure S16. In vitro biodegradation of the $P_{30}C_3T_3$ ($MBAm_{0.6}$) hydrogel in phosphate buffered saline (PBS) at 37 °C with 80 r.p.m shaking.
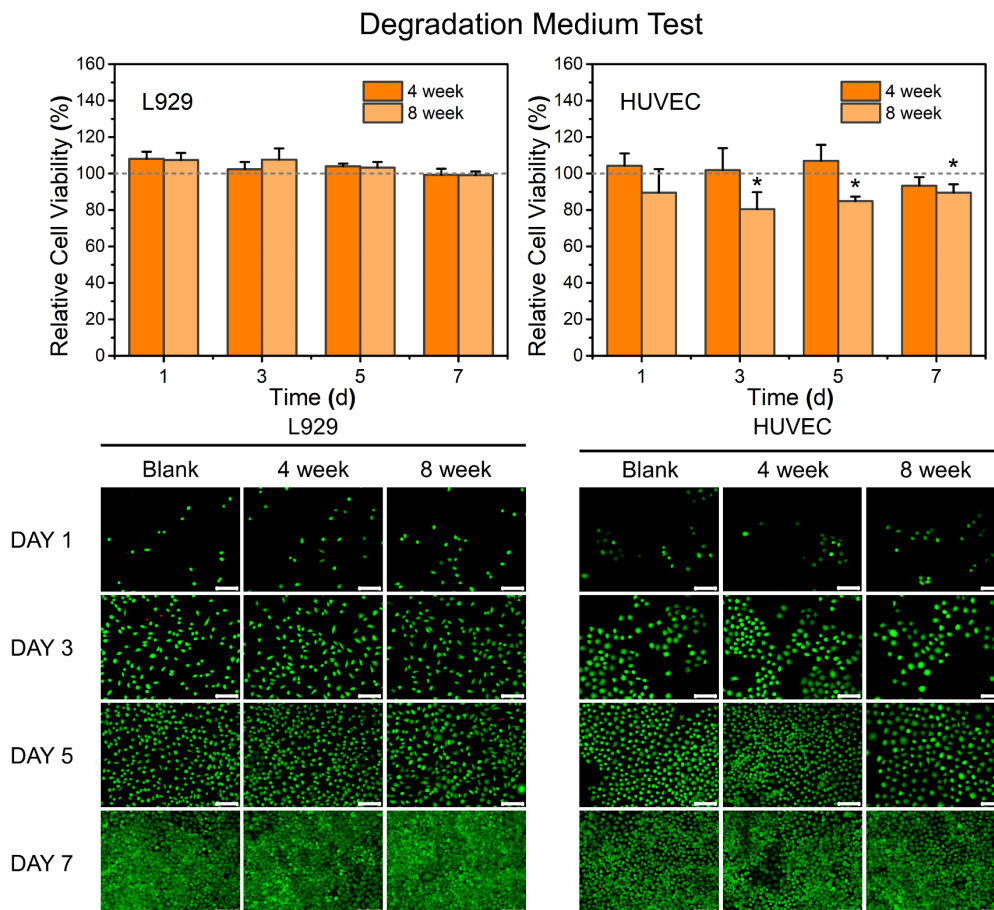
Figure S17. Relative viability and Live/dead fluorescence images of cell co-cultured with the degradation medium of the $P_{30}C_3T_3$ ($MBAm_{0.6}$) hydrogel. *$p < 0.05$, vs. the cell viability of the control group at the same time point. The scale bar in fluorescence images represents 100 μm.
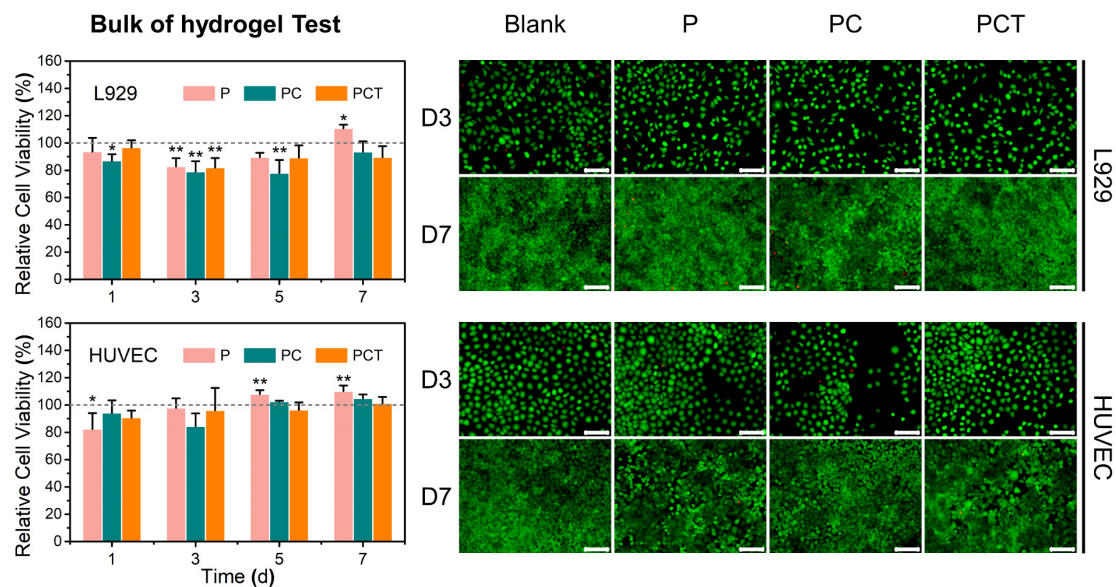
Figure S18. Relative viability and Live/dead fluorescence images of cell co-cultured with the bulk of hydrogels. *$p < 0.05$, **$p < 0.01$, vs. the cell viability of the control group at the same time point. The scale bar in fluorescence images represents 100 μm.
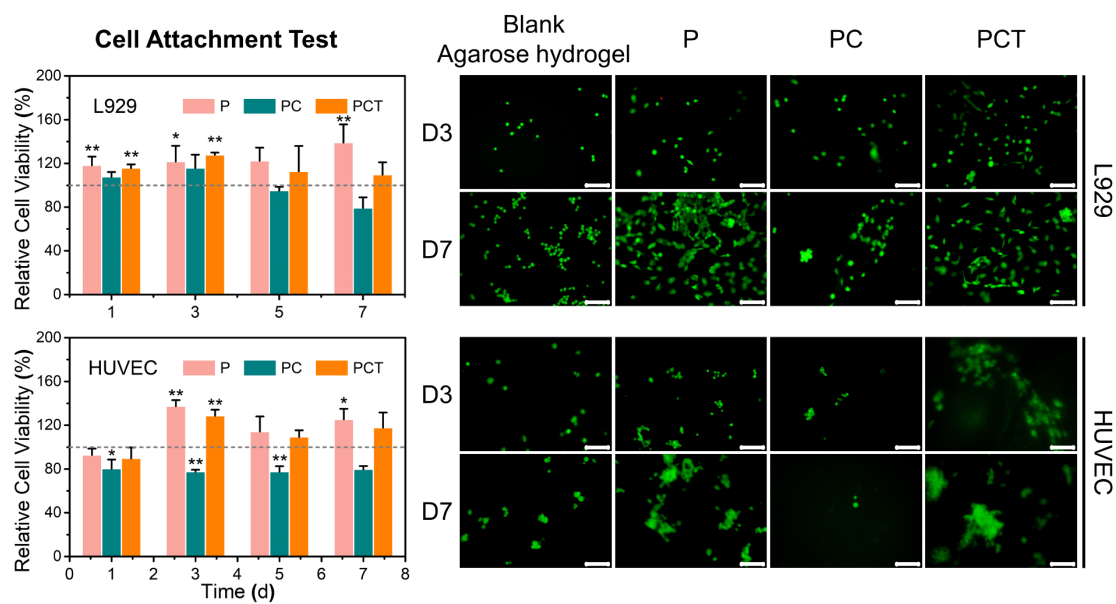
Figure S19. Relative viability and Live/dead fluorescence images of cell cultured on the surface of hydrogel matrixes. *$p < 0.05$, **$p < 0.01$, vs. the cell viability of the control group at the same time point. The scale bar in fluorescence images represents 100 μm.
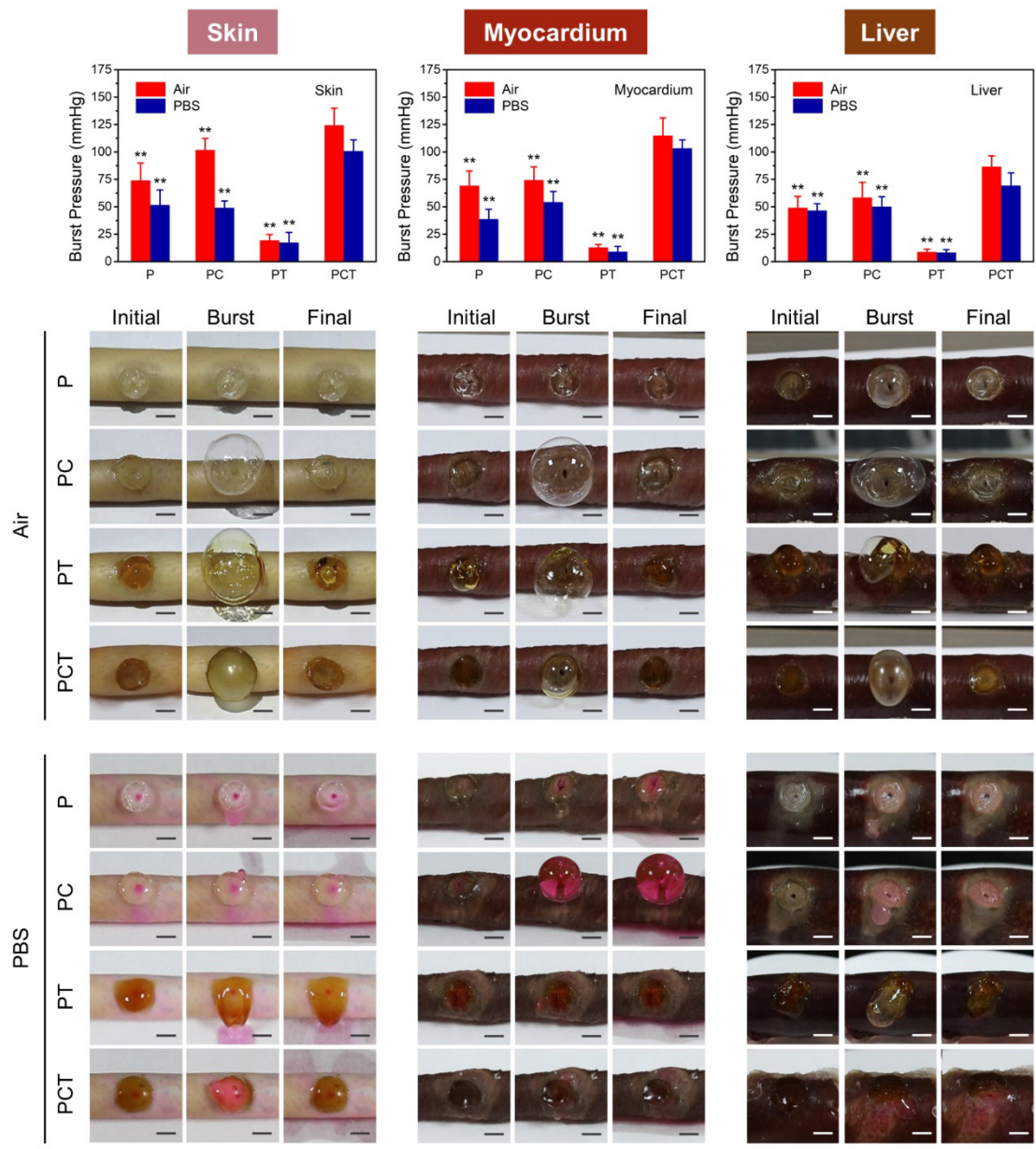
Figure S20. Burst pressure results and optical images of the hydrogel matrixes on the surface of porcine skin, myocardium and liver in air and PBS environment. **$p < 0.01$, vs. the burst pressure of the PCT hydrogel group at the same tested tissue substrate. The scale bar in optical images represents 5 mm.

Supplementary Movie Captions
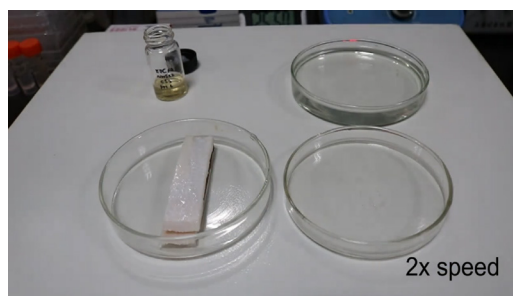
Movie S1: Preparation of hydrogel-tissue adhesive interface. Porcine skin was used as a representative tissue for demonstration.
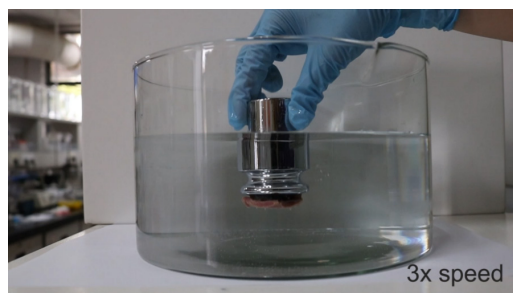
Movie S2: Direct and repeatable adhesion test of the $P_{30}C_3T_3$ ($MBAm_{0.6}$) hydrogel between stainless steel substrate and porcine myocardium in a PBS environment.

Movie S3: The $P_{30}C_3T_3$ ($MBAm_{0.6}$) hydrogel still adhered firmly to the surface of porcine skin after being washed by a high-pressure liquid.

Movie S4: The sealing effect of the $P_{30}C_3T_3$ ($MBAm_{0.6}$) hydrogel on the water leakage by a blocking test.

References

1   Q. B. Wei, F. Fu, Y. Q. Zhang and L. Tang, *J. Polym. Res.*, 2015, **22**(2), 15.

2   X. Su, Y. Luo, Z. L. Tian, Z. Y. Yuan, Y. M. Han, R. F. Dong, L. Xu, Y. T. Feng, X. Z. Liu and J. Y. Huang, *Mater. Horizons*, 2020, **7**(10), 2651−2661.

3   S. Mishra, G. Usha Rani and G. Sen, *Carbohydr. Polym.*, 2012, **87**(3), 2255−2262.

4   R. Baigorri, J. M. García-Mina and G. González-Gaitano, *Colloid Surf. A-Physicochem. Eng. Asp.*, 2007, **292**, 212−216.

5   A. G. Yavuz, A. Uygun and V. R. Bhethanabotla, *Carbohydr. Polym.*, 2009, **75**(3), 448−453.

6   S. Anwar, M. Mubarik, A. Waheed and S. Firdous, *Optik*, 2015, **126**, 871−876.

7   S. A. Riyajan and W. Sukhlaaied, *Mater. Sci. Eng. C*, 2013, **33**(3), 1041−1047.

8   M. P. Devi, M. Sekar, M. Chamundeswari, A. Moorthy, G. Krithiga, N. S. Murugan and T. P. Sastry, *Bull. Mater. Sci.*, 2012, **35**(7), 1157−1163.

9   S. Ghahri, B. Mohebby, A. Pizzi, A. Mirshokraie and H. R. Mansouri, *J. Polym. Environ.*, 2017, **26**(5), 1881−1890.

10 Z. Xia, A. Singh, W. Kiratitanavit, R. Mosurkal, J. Kumar and R. Nagarajan, *Thermochim. Acta*, 2015, **605**, 77−85.

11 H. Fan, J. Wang and J. P. Gong, *Adv. Funct. Mater.*, 2020, **31**(11), 2009334.

12 L. Han, M. Wang, L. O. Prieto-López, X. Deng and J. Cui, *Adv. Funct. Mater.*, 2019, **30**(7), 1907064.

13 Z. Yu and P. Wu, *Mater. Horizons*, 2021, **8**(7), 2057−2064.

14 C. Cui, T. Wu, X. Chen, Y. Liu, Y. Li, Z. Xu, C. Fan and W. Liu, *Adv. Funct. Mater.*, 2020, **30**(49), 2005689.

15 F. Pan, S. Ye, R. Wang, W. She, J. Liu, Z. Sun and W. Zhang, *Mater. Horizons*, 2020, **7**(8), 2063−2070.

16 L. Xu, S. Gao, Q. Guo, C. Wang, Y. Qiao and D. Qiu, *Adv. Mater.*, 2020, **32**(52), 2004579.

17 J. N. Lee, S. Y. Lee and W. H. Park, *ACS Appl Mater Interfaces*, 2021, **13**(15), 18324−18337.

18 H. Yuk, C. E. Varela, C. S. Nabzdyk, X. Mao, R. F. Padera, E. T. Roche and X. Zhao, *Nature*, 2019, **575**(7781), 169−174.